Cloud Feedback Processes in a General Circulation Model

R. T. WETHERALD AND S. MANABE

Geophysical Fluid Dynamics Laboratory/NOAA, Princeton University, Princeton, New Jersey

(Manuscript received 6 April 1987, in final form 30 November 1987)

ABSTRACT

The influence of the cloud feedback process upon the sensitivity of climate is investigated by comparing the behavior of two versions of a climate model with predicted and prescribed cloud cover. The model used for this study is a general circulation model of the atmosphere coupled with a mixed layer model of the oceans. The sensitivity of each version of the model is inferred from the equilibrium response of the model to a doubling of the atmospheric concentration of carbon dioxide.

It is found that the cloud feedback process in the present model enhances the sensitivity of the model climate. In response to the increase of atmospheric carbon dioxide, cloudiness increases around the tropopause and is reduced in the upper troposphere, thereby raising the height of the cloud layer in the upper troposphere. This rise of the high cloud layer implies a reduction of the temperature of the cloud top and, accordingly, of the upward terrestrial radiation from the top of the model atmosphere. Thus, the heat loss from the atmosphere–earth system of the model is reduced. As the high cloud layer rises, the vertical distribution of cloudiness changes, thereby affecting the absorption of solar radiation by the model atmosphere. At most latitudes the effect of reduced cloud amount in the upper troposphere overshadows that of increased cloudiness around the tropopause, thereby lowering the global mean planetary albedo and enhancing the CO_2 induced warming.

On the other hand, the increase of low cloudiness in high latitudes raises the planetary albedo and thus decreases the CO_2 induced warming of climate. However, the contribution of this negative feedback process is much smaller than the effect of the positive feedback process involving the change of high cloud.

The model used here does not take into consideration the possible change in the optical properties of clouds due to the change of their liquid water content. In view of the extreme idealization in the formulation of the cloud feedback process in the model, this study should be regarded as a study of the mechanisms involved in this process rather than the quantitative assessment of its influence on the sensitivity of climate.

1. Introduction

It has been noted that cloud cover can exert a large influence upon climate (for example, see Manabe and Wetherald 1967; and Schneider 1972). For example, cloud cover reflects a large fraction of incoming solar radiation, thereby decreasing the solar energy absorbed by the earth–atmosphere system. On the other hand, cloud cover lowers the temperature of the effective source for the outgoing terrestrial radiation and decreases the loss of energy from the system. Since the magnitudes of these two opposing effects often differ substantially from each other, the change in the distribution of cloud cover can have a large effect upon the sensitivity of climate. This is why many studies have been conducted on the influence of the cloud feedback process upon the sensitivity of climate. For example, Cess (1976), Hartmann and Short (1980) and Ohring and Clapp (1980) investigated the influence of cloud cover upon the radiation balance of the earth–atmosphere system based upon the data from meteorological satellites. Wetherald and Manabe (1980) and Hansen et al. (1984) investigated how the interaction between cloud cover and radiative transfer affects the sensitivity of a model climate.

The study of Wetherald and Manabe (1980) indicated that the cloud feedback process in their model has very little effect upon the sensitivity of climate to a forcing such as a change of solar constant or that of atmospheric carbon dioxide. On the other hand, the recent study of Hansen et al. (1984) suggests that it markedly enhances the surface warming induced by the doubling of atmospheric carbon dioxide. Despite such a difference, the features of cloud cover change obtained in these two studies, as well as in the recent study of Washington and Meehl (1984), qualitatively resemble each other as noted by Wetherald and Manabe (1986). Therefore, it appears worthwhile to conduct an in-depth analysis of the results from a climate sensitivity study and identify some of the basic mechanisms which control the CO_2-induced change of cloud cover and its effect upon the sensitivity of climate. This study represents an attempt to do this by use of the results from the climate model recently developed at

Corresponding author address: Dr. Richard T. Wetherald, Geophysical Fluid Dynamics Laboratory, Princeton University, P.O. Box 308, Princeton, NJ 08542.

the Geophysical Fluid Dynamics Laboratory of NOAA (Manabe and Broccoli 1985). It is hoped that the study also may lead to the development of an effective research strategy for the improved modeling of the cloud feedback process.

The present paper begins with descriptions of two climate models, with and without the cloud feedback process, followed by a comparison of the sensitivities of these two models. It proceeds to a description of the CO_2-induced changes of cloud cover and a discussion of the mechanisms responsible for such changes. The magnitudes of various feedback processes are determined to estimate the relative importance of the cloud feedback process on the sensitivity of the model climate. This is followed by a detailed analysis of the influence of change of cloud distribution upon the radiative fluxes. The results from this analysis are compared with those from other numerical experiments. The paper concludes with an assessment of the results from the present study and its implication for future research.

2. Description of the model

a. Structure

The mathematical model of climate used for this research is an atmospheric general circulation model coupled with a static mixed layer ocean model (Manabe and Stouffer 1980). The atmospheric portion of the model constructed by Gordon and Stern (1982) predicts the changes of the vertical component of vorticity and the horizontal divergence, temperature, surface pressure and moisture based upon the equations of motion, the thermodynamical equation, and the continuity equations of mass and moisture. The horizontal distributions of these variables are represented by a limited number of spherical harmonics, namely, the first 15 modes in the zonal direction and the same number of degrees of freedom in the meridional direction for each wavenumber. The vertical distributions are specified at nine unequally spaced finite difference levels. The model has a global computational domain, realistic orography and land–sea contrast and seasonally varying insolation.

In the dynamical computation described here, the transform method (e.g., Orsag 1970) is used. In this method the appropriate spectral variables are transformed to gridpoint values on a horizontal grid of a designated resolution. The nonlinear terms of the dynamical equations are evaluated on this grid and the results of these computations are transformed back into the spectral domain.

Precipitation is computed whenever supersaturation is indicated by the prognostic equation for water vapor. It is identified as snowfall when the air temperature near the surface falls below freezing; otherwise it is identified as rain. The moist convective processes are parameterized by a moist convective adjustment scheme as proposed by Manabe et al. (1965).

The temperature of the continental surface is determined so that it satisfies the condition of local thermal equilibrium among the various components of surface heat balance. A change in snow depth is computed as a net contribution from snowfall, sublimation and the snowmelt which is determined from the requirement of surface heat balance (see Manabe 1969 for further details). The soil albedo is prescribed geographically but is replaced by a higher value over snow-covered regions.

The distribution of insolation is seasonally (but not diurnally) prescribed at the top of the model atmosphere. The method for computing solar radiation is similar to that proposed by Lacis and Hansen (1974). Terrestrial radiation is computed by a modified version of the method described by Rodgers and Walshaw (1966) and includes the effect of the water vapor continuum. The mixing ratio of carbon dioxide is taken to be constant everywhere (300 ppm). Ozone is specified as a function of latitude, height and season. The distribution of water vapor is determined from the prognostic equation of water vapor.

In order to facilitate the analysis and interpretation of the results from the numerical experiment, the prognostic scheme of cloud cover is made as simple as possible. At each gridpoint, cloud is placed in the layer where the relative humidity exceeds a critical value. Otherwise no cloud is forecast. This value for the critical relative humidity (99%) is chosen so that the global integral of total cloud amount is approximately 50%. In the present scheme, cloud may occur in a single or at multiple contiguous vertical layers. If the cloud is more than one layer thick, it is regarded as a thick cloud. In this study, the same critical relative humidity is used for both large scale and convective clouds.

The fractional absorption and reflection of solar radiation by various types of cloud cover are determined by referring to the study by Rodgers (1967) and are tabulated in Table 1. For the computation of terrestrial radiation, all clouds except "cirrus" or high clouds are assumed to be completely black. The latter cloud type is taken to be 60% black based upon data compiled by Kondratiev (1972). Other aspects of the cloud prediction scheme are discussed in more detail in Wetherald and Manabe (1980). It should be mentioned that the model does not compute cloud liquid water content and, therefore, the effect of varying optical depth of clouds is not taken into account in this study. For the sake of simplicity, it is assumed that all condensed water vapor immediately precipitates out of the model atmosphere despite the fact that cloud cover is placed whenever relative humidity exceeds the critical value.

The oceanic portion of the model is a static isothermal layer of sea water with a uniform thickness of 50 meters. The ocean temperature change is computed from the budget of surface heat fluxes. The effects of

TABLE 1. Optical properties of cloud cover in the models used in the present study. Here "thin cloud" indicates a cloud which occupies only one finite difference level, while "thick cloud" indicates a cloud which occupies more than one contiguous finite difference level. "Visible and UV" denotes solar radiation with wavelength less than 0.7 μm, whereas "near-infrared" indicates the part of solar spectrum with wavelength longer than 0.7 μm.

Cloud type		Approximate height (km)	Solar				Longwave emissivity (%)
			Reflectivity (%)		Absorptivity (%)		
			Visible + UV	Near-infrared	Visible + UV	Near-infrared	
Thin cloud	High	10.5–∞	21	19	0	4	60
	Middle	4.0–10.5	45	35	0	30	100
	Low	0.0–4.0	65	55	0	30	100
Thick cloud		0.0–∞	65	55	0	30	100

horizontal heat transport by ocean currents and heat exchange between the mixed layer and the deeper layer of the ocean are neglected. The changes in sea ice thickness are computed from the processes of melting and freezing of ice, sublimation and snowfall as proposed by Bryan (1969). The ocean albedo is prescribed as a function of latitude but is replaced by a higher value over oceanic regions covered by sea ice.

b. Standard simulation

This section will briefly describe the simulation of two relevant quantities from the standard integration of the model. Figure 1 shows the latitudinal distribution of the zonal mean surface air temperature along with the observed values taken from Crutcher and Meserve (1970) and Taljaard et al. (1969). In general, the agreement is quite good for most latitudes except in the Southern Hemisphere at around 60°S and from 75° to 90°S where the computed values are too warm.

Figure 2 compares the simulated distribution of the deviation of zonal mean surface air temperature from its annual mean value with the distribution of the corresponding quantity for the actual atmosphere (Crutcher and Meserve 1970; Taljaard et al. 1969). This figure indicates that the amplitude and phase of the seasonal variation of surface air temperature are reasonably well simulated, although the amplitude of the computed seasonal variation is somewhat larger than that observed at around 60° latitude in both the Northern and Southern hemispheres. Although the surface temperatures between 75° and 90°S latitude are too warm throughout the entire year, the greatest deviation from the observed values occurs during the fall season.

The amount of cloud cover computed by the model is another important quantity for this investigation. Figure 3 illustrates the latitude–time variation of zonal mean total cloud amount for the model along with corresponding observations of this quantity taken from Berlyand and Strokina (1980). Here it is noted that there is a considerable seasonal variation of cloud cover computed by the model in middle to high latitudes in both hemispheres which is not evident in the observations. In particular, cloud cover is greatest during the winter season and smallest during the summer season, whereas there is a very little seasonal variation in these latitudes in the observed cloud data of Berlyand and Strokina. One of the shortcomings of the present simulation of cloud cover is a systematic underestimate of low stratiform cloud cover over the ocean in high latitudes of both hemispheres and off the western coastlines of the major continents during the summer seasons. These features have been illustrated in a previous publication (Manabe and Wetherald 1982) and undoubtedly contribute to the overall underestimation of cloud cover from middle to high latitudes. On the other hand, both the annual mean and seasonal variation of cloud cover appear to be reasonably well simulated from 40°N to 40°S latitude.

Despite the shortcomings of the computed cloud distribution shown in Fig. 3, the computed planetary

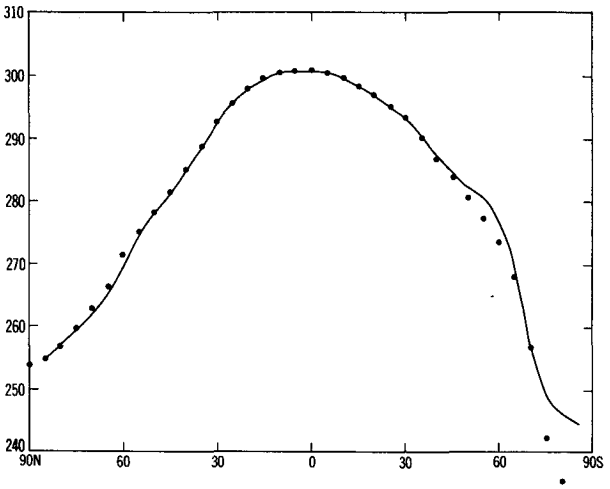

FIG. 1. Annually averaged, zonal mean surface air temperature (°K) for the model. Dots denote observed values from Crutcher and Meserve (1970) and Taljaard et al. (1969).

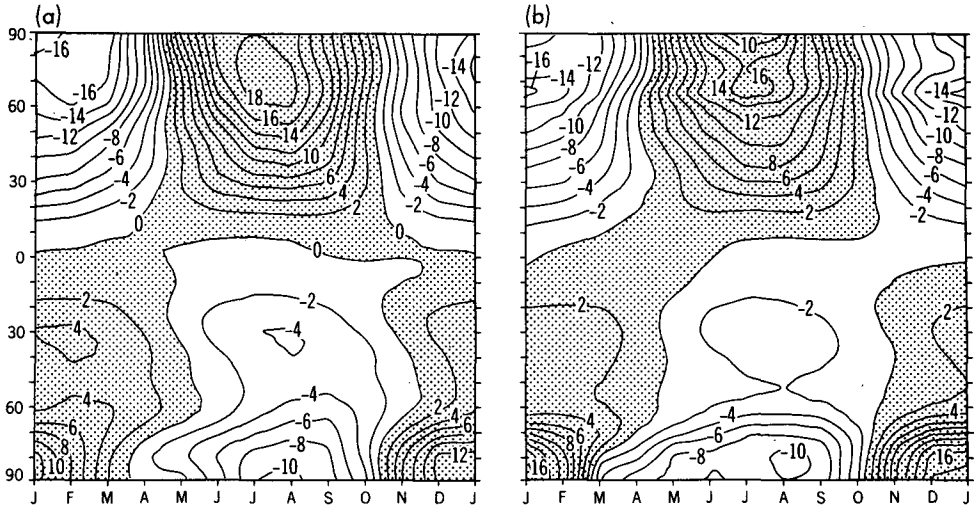

FIG. 2. Latitude–time distribution of the deviation in zonal mean surface air temperature from its annual mean value (°K): (a) computed distribution from the model, (b) observed distribution compiled by Crutcher and Meserve (1970) and Taljaard et al. (1969).

albedo appears to compare quite favorably with observation. Figure 4 shows the latitude–time distribution of zonal mean planetary albedo, both computed and observed. The observed distribution is taken from data presented in Ellis and Vonder Haar (1976). In general, the correspondence between the computed and observed values is good for most latitudes including the tropics and polar regions. Exceptions to this are the latitude regions of 45°–55°N during July and August and 55°–65°S where the computed planetary albedo is considerably less than the observed values. This is due to the underestimation of cloud cover over the oceans in these regions, as mentioned previously.

3. Sensitivity experiments

In order to evaluate the influence of the cloud feedback process upon the sensitivity of climate, two climate models are constructed. The first model predicts the distribution of cloud cover and thereby incorporates the interaction between cloud cover and radiative transfer in the atmosphere. It is described in section 2b and is identified as the global, variable-cloud-cover (GVC) model. The second model, identified as the global, prescribed-cloud-cover (GPC) model, is the same as the first except that the distribution of cloud cover is prescribed as described here. Thus, it does not have the cloud feedback process.

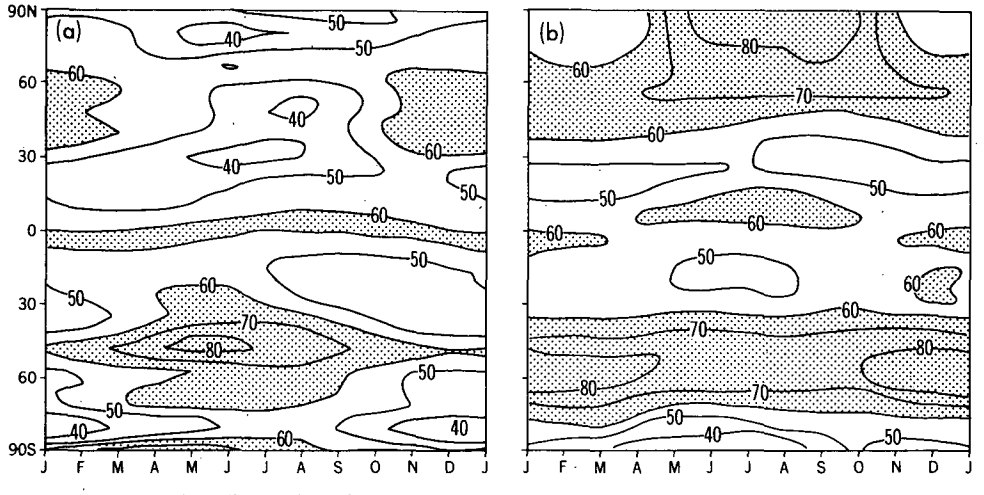

FIG. 3. Latitude–time distribution of the zonal mean total cloud amount (%): (a) computed distribution from the model, (b) observed distribution compiled by Berlyand et al. (1980).

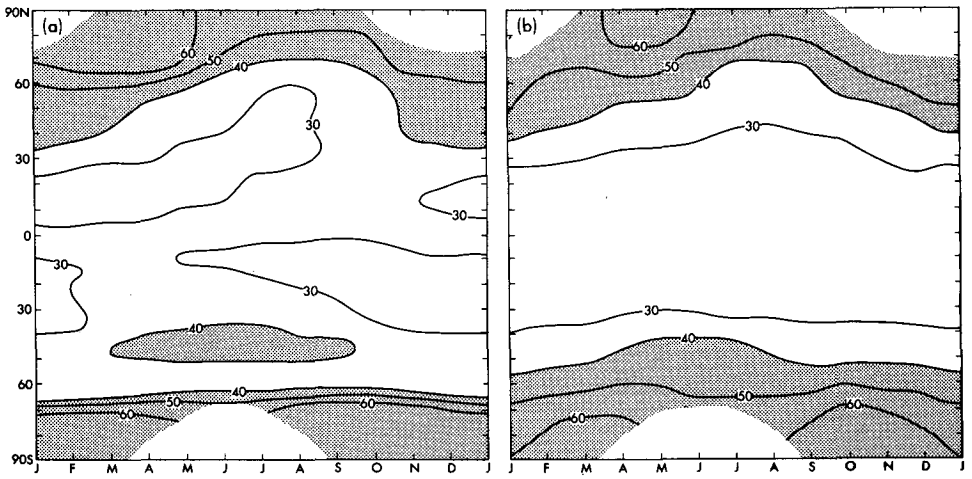

FIG. 4. Latitude–time distribution of the zonal mean planetary albedo (%): (a) computed distribution from the model, (b) observed distribution compiled by Ellis and Vonder Haar (1976).

With these models two sets of numerical integrations are conducted. The first set consists of the two time integrations of the GVC model in which the atmospheric concentration of carbon dioxide is prescribed to be 300 and 600 ppm by volume, respectively. Starting from the initial condition of an isothermal and dry atmosphere at rest and an isothermal mixed layer ocean, a numerical integration for each experiment is conducted over a period of 40 years. To accelerate the approach towards an equilibrium, the so-called asynchronous integrations of atmospheric and oceanic components of the model are conducted as described by Manabe and Stouffer (1980) during the first 10 years of the approach. Towards the end of each time integration, no systematic trend is noted in the temporal variation of the model climate. The climatic effect of the doubling of the atmospheric carbon dioxide is evaluated by comparing the two time mean states obtained from the time integrations with the normal and twice-normal concentrations of atmospheric carbon dioxide.

In the second set of integrations, the GPC model with the prescribed cloud cover is used. The distribution of cloud obtained from the last year of the integration of the GVC model with the normal CO_2 concentration is repeatedly cycled through these integrations. Otherwise, the procedures of the integrations are identical with those of the first set described in the preceding paragraph. By comparing the alterations of the climates of the GVC and GPC models induced by the doubling of the atmospheric carbon dioxide, the influence of the cloud feedback process upon the sensitivity of climate is investigated.

Figure 5 compares the zonally and annually averaged thermal responses of the GVC and GPC models to the doubling of atmospheric carbon dioxide. According to this figure the sensitivity of surface air temperature of the GVC model is considerably greater than that of the GPC model except in high latitudes of the Southern Hemisphere where it is very similar. Table 2 lists the global mean increases of surface air temperature obtained from the two models. According to this table the increase of surface air temperature for the GVC model is 1.25 times that of the GPC model. On the other hand, the decrease of zonal mean temperature in the model stratosphere is very similar for both models. This implies that the stratospheric cooling due to the additional CO_2 is relatively unaffected by the inclusion of the cloud feedback mechanism. Since the vertical heat exchange between the stratosphere and troposphere is much smaller than the exchange in the troposphere itself, this result is to be expected.

4. Changes in cloud cover

a. Annual mean change

Figure 6 illustrates the CO_2-induced change of zonal mean cloud amount computed from the GVC model. Some of the features of cloud change include

1) a reduction of cloud amount in the upper troposphere in middle and low latitudes;
2) an increase of cloud amount around the tropopause for all latitudes, particularly in high latitudes;
3) an increase of cloud amount in the stable region near the model surface in higher latitudes.

According to a recent review article by Wetherald and Manabe (1986), qualitatively similar features are detectable in the CO_2-induced change of cloud cover obtained from various models constructed at GFDL and other institutions. These alterations of cloud cover translate into the change of total cloud illustrated in Fig. 7. This figure indicates that total cloud amount

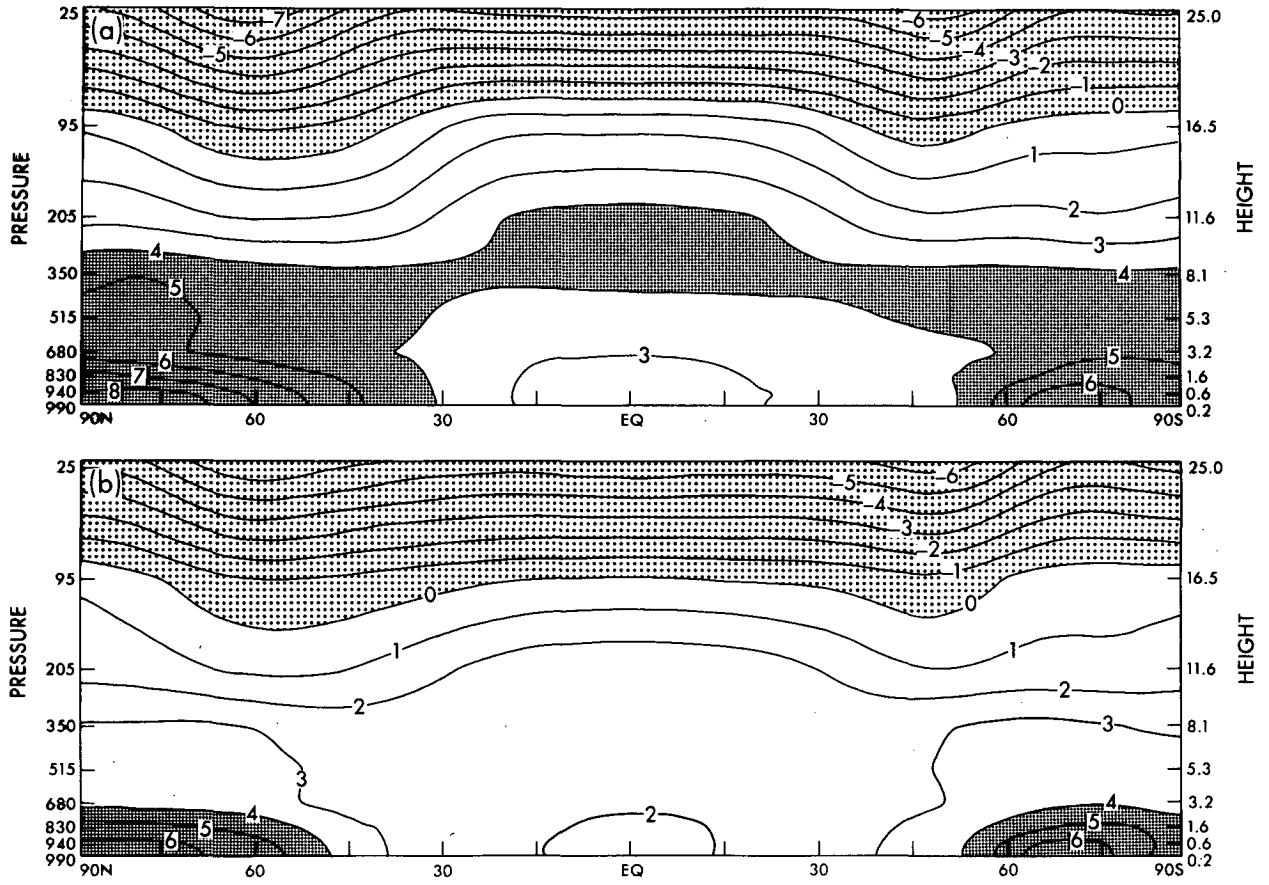

FIG. 5. Latitude–height distribution of the CO_2-induced change of zonal mean temperature (°K) obtained from the (a) GVC model and (b) GPC model.

decreases equatorwards of approximately 40° latitude in both hemispheres and increases polewards of this latitude.

To appreciate the implication of the CO_2-induced change of cloud cover described here, it is useful to inspect first the distribution of zonal mean cloud amount which is obtained from the standard experiment as shown in Fig. 6b. This figure indicates that a thick layer of relatively large cloudiness exists in the upper troposphere of the model. The altitude of this high cloud layer decreases with increasing latitudes in a manner similar to the height of the tropopause. This suggests that the tropopause and the upper tropospheric layer beneath it serve as a lid to the upward motion which is responsible for the formation of the cloud layer in the upper model troposphere.

In a quasi-geostrophic system the vertical velocity can be determined diagnostically from the ω-equation (for example, see Holton 1979). One can infer from this equation that the vertical velocity depends strongly upon the static stability of the atmosphere and tends to become weaker with increasing stability. In a saturated environment where cloud forms, the effective static stability can be evaluated by computing the moist (rather than dry) static stability. Figure 8 illustrates the latitude–height distribution of this quantity which is defined as the vertical derivative of equivalent potential temperature θ_{es}, i.e.,

$$\theta_{es} = \theta \exp \frac{Lr_s(T)}{C_p T},$$

where θ is the potential temperature, T the absolute temperature, r_s the saturation mixing ratio of water vapor in air, L the latent heat of condensation, and C_p the specific heat of air under constant pressure. For reference, the layers where the zonal mean cloudiness

TABLE 2. Increases of global mean surface air temperatures of GVC and GPC models. Units are in °C.

Model	Cloud cover	Temperature increase
GVC	Predicted	4.0
GPC	Prescribed	3.2

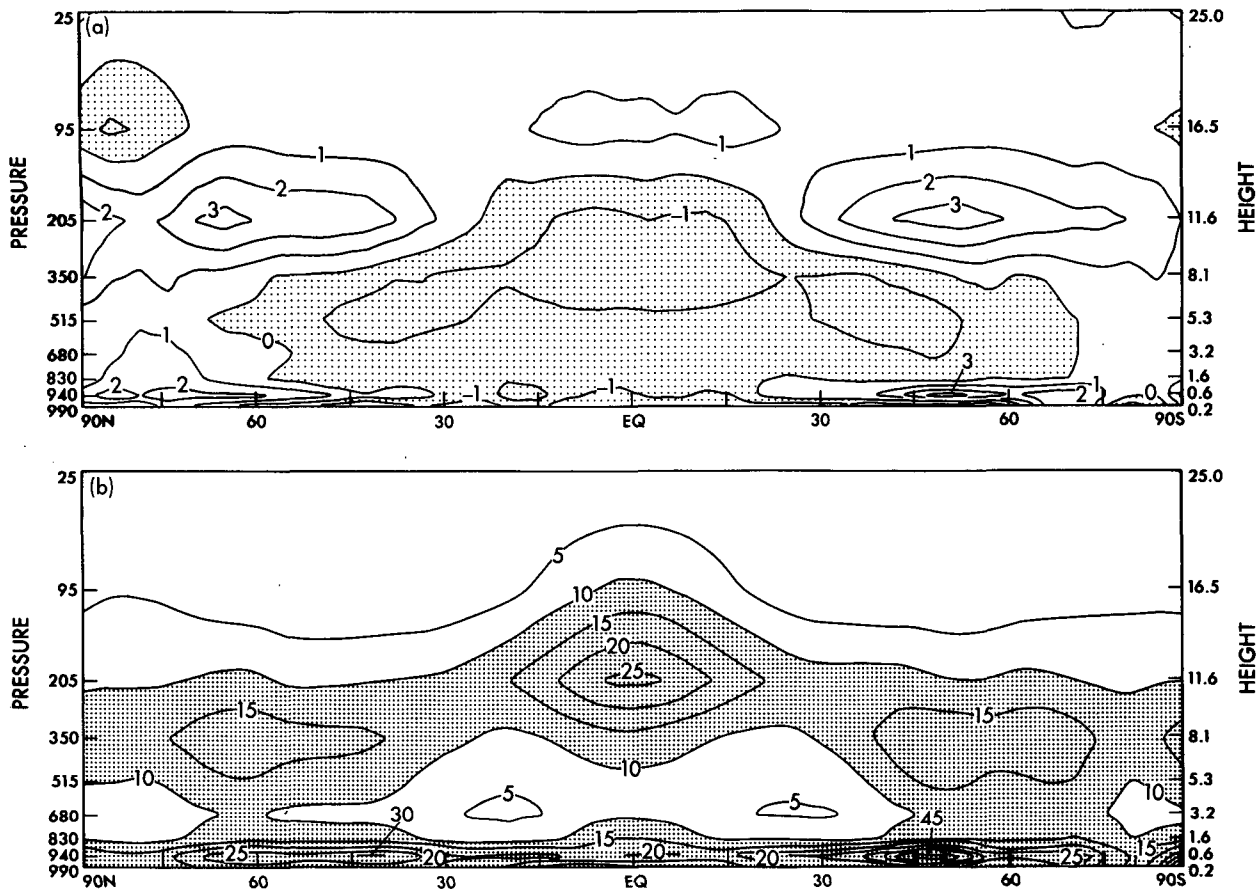

FIG. 6. Latitude–height distribution of (a) CO_2-induced change of zonal mean cloud amount (%), (b) zonal mean cloud amount (%) obtained from the GVC model.

is more than 10% are shown shaded in Fig. 8. According to this figure, the upper tropospheric level of high cloudiness is located at the level where the moist static stability begins to increase sharply with increasing altitude. As saturated air reaches this level and loses its upward velocity, it tends to spread horizontally. Thus, cloud cover also spreads in an anvil-like manner over an extensive area in the upper model troposphere. This is in contrast to the situation in the middle troposphere where the variance of vertical velocity is larger and the cloud-free region with downward motion occupies a larger fraction of the area. Accordingly, the total cloud amount in the upper troposphere is much larger than in the middle troposphere.

When one compares the distribution of the high cloud described here with that of the CO_2-induced change of zonal mean cloud amount shown in Fig. 6a, one notes that cloud amount increases in the upper part of this cloud region, whereas it is reduced in the lower part. This implies that the altitude of the high cloud in the upper model troposphere increases in response to the doubling of atmospheric carbon dioxide.

To explore the mechanism responsible for this upward shift of high cloud, the vertical profiles of moist static stability at 50°N obtained from both the standard and high CO_2 experiments are illustrated in Fig. 9a. For reference, the vertical distributions of zonal mean cloudiness from these two experiments are also shown

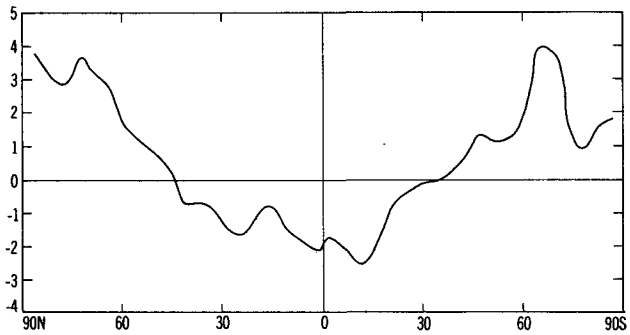

FIG. 7. Latitudinal distribution of the CO_2 induced change of zonal mean total cloud amount (%) for the GVC model.

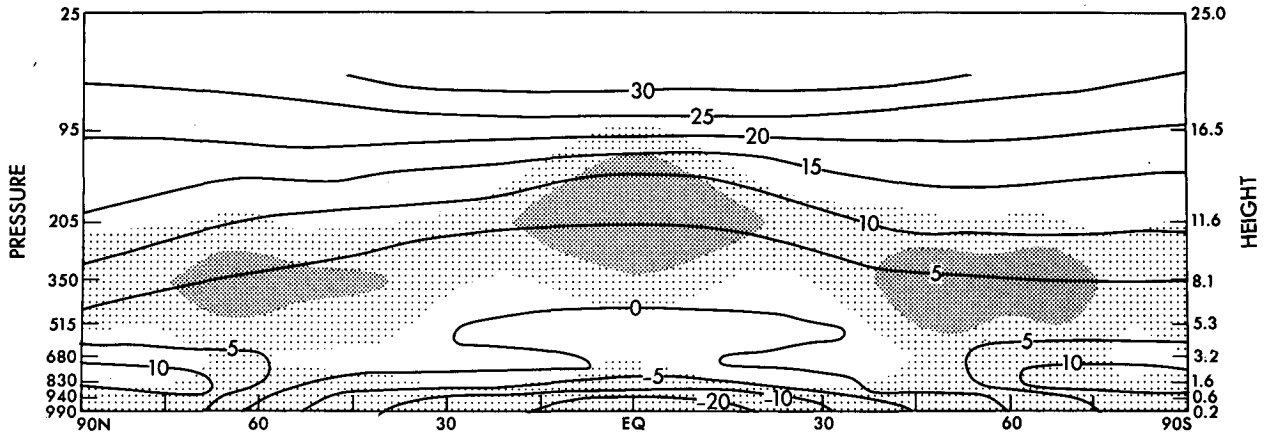

FIG. 8. Latitude–height distribution of the moist static stability for the standard integration of the GVC model (°C km^{-1}). Shaded areas superimposed upon this distribution denote regions where the zonal mean cloud amount exceeds 10% (light shade) and 20% (dark shade). The 20% or greater regions near the model surface are not shaded to emphasize the features in the upper model atmosphere.

in Fig. 9b. In both experiments the moist static stability in the lower and middle troposphere has a small positive value but increases sharply with increasing altitude in the upper model troposphere where the high cloud layer is located. When one compares the vertical profiles of moist static stability from the two experiments, one notes that the profile shifts upwards in response to the doubling of the atmospheric concentration of carbon dioxide. This implies a rise of the cloudy layer of the upper troposphere where the moist static stability sharply increases with increasing altitude and saturated, ascending air spreads horizontally. Similar upward shifts of the moist static stability profile occur at other latitudes. Although the spacing of the vertical finite difference levels is too large to determine the level of maximum cloudiness from Fig. 9b, the upward shift

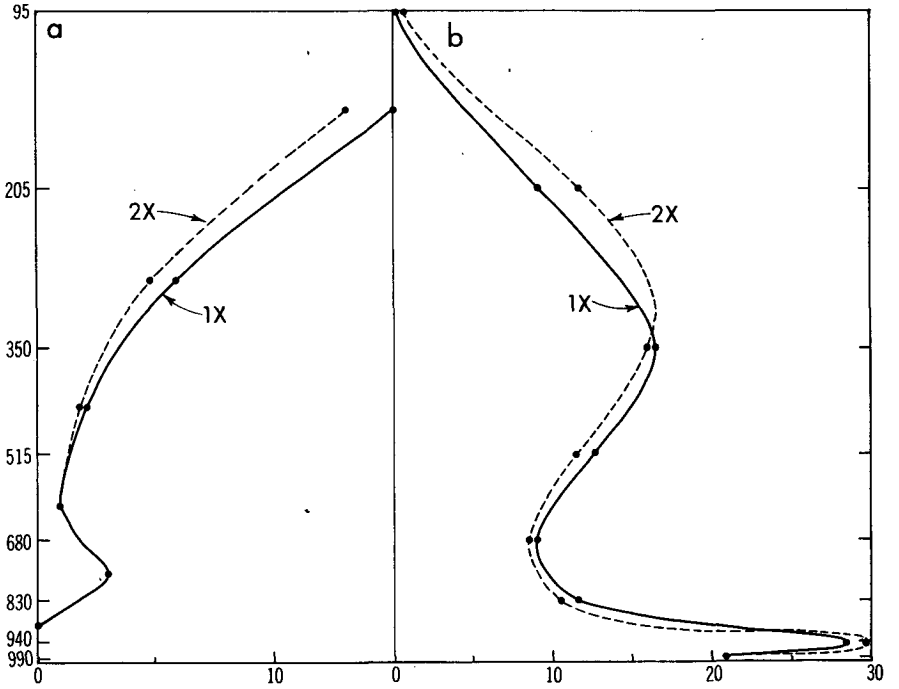

FIG. 9. Vertical profiles at 50°N latitude of (a) moist static stability (°C km^{-1}) and (b) zonal mean cloudiness (%) obtained from both standard and high-CO_2 integrations of the GVC model.

of the cloud layer may be clearly inferred from the relative placement of the solid and dashed lines above and below the 350 mb level.

The upward shift of the moist stability profile as described appears to result from the enhancement of the moist convective activity in low and middle latitudes of the model. In response to an increase of atmospheric carbon dioxide, the global mean rate of evaporation increases as discussed by Manabe and Wetherald (1975), and the heating due to moist convection and large-scale condensation intensifies. Thus, the layer of relatively small, moist static stability (Fig. 8) becomes thicker, thereby shifting upwards the vertical profile of moist static stability.

In the model tropics where the static stability of the lower and middle troposphere is moist adiabatically unstable and the Coriolis force is small, one cannot use the ω-equation to discuss the distribution of vertical p-velocity. Instead, the entire vertical profile of static stability should be examined for this purpose. Figure 10a illustrates the vertical distribution of equivalent potential temperature θ_e defined by

$$\theta_e = \theta \exp\left(\frac{Lr}{C_pT}\right),$$

where r is the mixing ratio of air. This figure clearly indicates that a saturated air parcel originating from the planetary boundary layer can reach a higher altitude in the warm, high CO_2 atmosphere, thereby raising the altitude of the cloudy layer of the upper model troposphere (Fig. 10b).

In summary, the CO_2-induced changes of cloud amount in the upper model troposphere may be regarded as a manifestation of the rise of high cloud which is caused by the upward shift in the thermal structure of the model atmosphere. However, the CO_2-induced change of high cloudiness shown in Fig. 6 should not be regarded as a simple shape-preserving, upward shift of a cloud layer. Figure 9b indicates that, at 40°N, the increase of cloudiness around the tropopause is substantially larger than the reduction of cloud amount in the middle troposphere. On the other hand, the tropical cloudiness is reduced significantly over a very thick layer of the upper troposphere as Figs. 6a and 10b indicate. These results indicate that, as the high cloud layer shifts upward towards the model tropopause, its vertical cloudiness profile is altered. One also notes that the reduction of cloudiness extends into the middle model troposphere though its magnitude is smaller. So far, it has not been possible to satisfactorily identify the physical mechanisms responsible for the change of the vertical cloudiness profile.

The mechanism of the CO_2-induced change of cloud cover described here is different from that suggested previously by Wetherald and Manabe (1980). In that earlier study, the reduction of cloud cover in the troposphere was attributed to the enhanced removal of

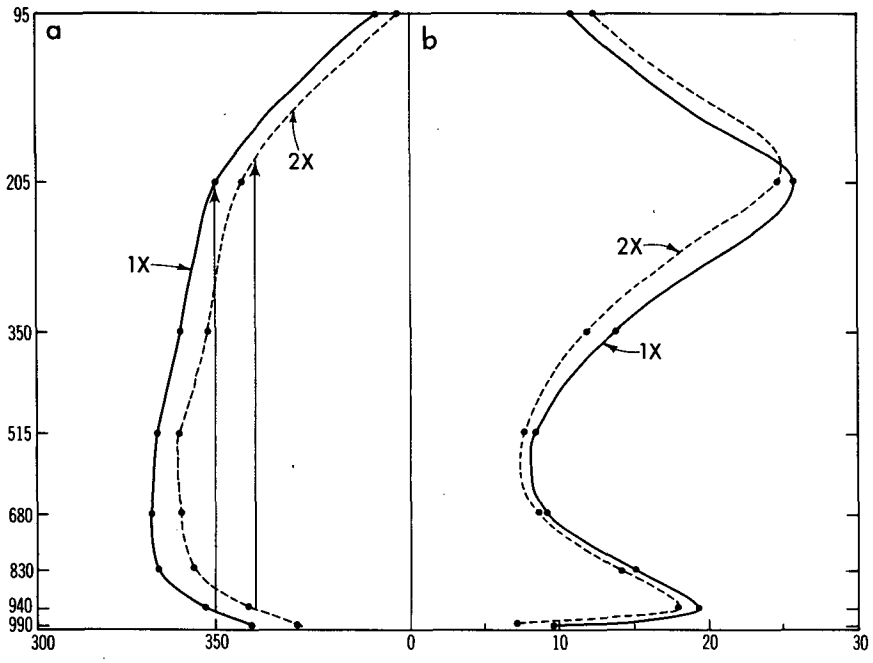

FIG. 10. Vertical profiles at the equator of (a) equivalent potential temperature (°C) and (b) zonal mean cloudiness (%) obtained from both the standard and high-CO_2 integrations of the GVC model. The vertical lines with arrowheads denote a vertical ascent of a saturated air parcel originating from the planetary boundary layer in both model atmospheres.

moisture due to the intensification of the vertical velocity. In the present study, the layer in which the zonal mean variance of the vertical velocity increases does not necessarily coincide with the layer of reduced relative humidity in middle latitudes. Therefore, it has not been possible to demonstrate convincingly the relevance of this mechanism to the general reduction of tropospheric relative humidity in middle and low latitudes. Unfortunately, neither mechanism can explain satisfactorily the details of the latitude–height distribution of the CO_2-induced change of tropospheric cloudiness.

So far, the discussion has centered around the CO_2-induced change of cloud cover in the upper model troposphere and around the tropopause. However, Fig. 6a also indicates that the amount of low cloud near the earth's surface in high latitudes also increases in response to the doubling of the atmospheric carbon dioxide. As noted by Wetherald and Manabe (1980), the warming of the earth's surface contributes to a reduction of "Bowen's ratio"; i.e., the ratio of sensible to latent heat fluxes into the atmosphere. A high nonlinear increase of saturation vapor pressure with increasing surface temperature enhances evaporation and is responsible for this reduction. Since the warming is at a maximum at the earth's surface and sharply decreases with increasing altitude, it is expected that the enhanced evaporation from the underlying surface contributes to the increase of relative humidity at a level located slightly above the earth's surface. It is also reasonable that the increase of low cloud occurs in high latitudes where the lowest layer of the model atmosphere has a relatively stable stratification and tends to prevent the penetration of moist air towards higher levels.

b. Seasonal change

Figure 11 illustrates the seasonal variation of the CO_2-induced change of zonal mean total cloudiness. This figure indicates that, in middle and high latitudes, total cloudiness increases in winter, whereas it is reduced in summer responding to the doubling of the atmospheric concentration of carbon dioxide. Most of this summer reduction takes place over the continents in the lower model troposphere. In response to the doubling of atmospheric carbon dioxide, soil wetness and the cloudiness of the lower model troposphere are reduced over extensive continental regions in middle latitudes in summer. This subject was discussed in a separate study (Manabe and Wetherald 1987).

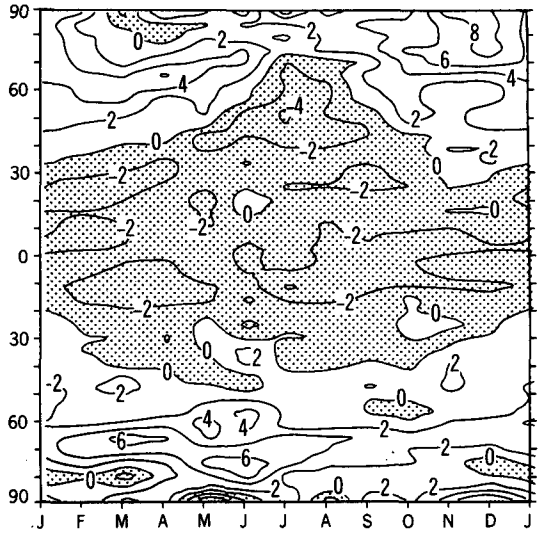

FIG. 11. Latitude–time distribution of the CO_2 induced change of total cloud amount (%) for the GVC model.

5. Feedback analysis

a. Formulation

This section evaluates how the sensitivities of the GVC and GPC models are affected by various feedback processes involving the basic variables such as cloud cover, temperature, water vapor and surface albedo. In order to do this, it is desirable first to obtain an expression that determines the influence of the change in each variable upon the radiation balance of the earth–atmosphere system.

When the atmosphere–mixed-layer ocean system of the model is in a thermal equilibrium state, the following condition should be satisfied at the top of the model atmosphere.

$$\tilde{R} = 0 \tag{5.1}$$

where the tilde denotes global average and R is the annually averaged, net downward flux of radiation at the top of the atmosphere; R may be subdivided into solar and terrestrial components as follows:

$$\tilde{R} = \tilde{S} - \tilde{F}, \tag{5.2}$$

where $\tilde{S}$ is the net downward solar radiation and $\tilde{F}$ is the upward terrestrial radiation at the top of the atmosphere. From Eq. (5.1), it follows that

$$\delta\tilde{R} = \delta\tilde{S} - \delta\tilde{F} = 0, \tag{5.3}$$

where δ denotes the difference between the thermal equilibrium with the normal and twice-normal concentrations of atmospheric carbon dioxide.

If the CO_2 perturbation of climate is sufficiently small, the following approximate expression holds:

$$\delta\tilde{R} \approx \delta_x\tilde{R} + \delta_T\tilde{R} + \delta_r\tilde{R} + \delta_A\tilde{R} + \delta_c\tilde{R} \tag{5.4}$$

where, for example,

$$\delta_x\tilde{R} = \tilde{R}(x + \delta x, T_i, r_i, A, C_i) - \tilde{R}(x, T_i, r_i, A, C_i) \tag{5.5}$$

$$\delta_T\tilde{R} = \tilde{R}(x, T_i + \delta T_i, r_i, A, C_i) - \tilde{R}(x, T_i, r_i, A, C_i). \quad (5.6)$$

Here, x and A denote the concentration of carbon dioxide and surface albedo, and T_i, r_i and C_i denote the temperature, mixing ratio of water vapor and cloud amount at all finite difference levels. Similarly δS and δF may be approximated by

$$\delta\tilde{S} \approx \delta_x\tilde{S} + \delta_r\tilde{S} + \delta_A\tilde{S} + \delta_c\tilde{S} \quad (5.7)$$

$$\delta\tilde{F} \approx \delta_x\tilde{F} + \delta_T\tilde{F} + \delta_r\tilde{F} + \delta_c\tilde{F}. \quad (5.8)$$

The computational procedure involved in obtaining the various components of δS and δF is briefly outlined as follows. The radiation algorithm of the model is used to compute the standard fluxes S_x, S_r, S_A, S_c, F_x, F_T, F_r and F_c at each gridpoint from 1) the seasonal mean values of temperature, water vapor and surface albedo and, 2) the daily values of cloudiness which are obtained from the (1 × CO_2) standard integration of the model. Since the time mean value of radiative flux emitted from the temporally varying cloud can differ significantly from the radiative flux emitted from the hypothetical clouds with a time mean distribution, daily (instantaneous) cloudiness is used for the computation of S_c and F_c. The fluxes thus obtained are then averaged over the global computational domain of the model. This radiative computation is then repeated for each term by replacing, in succession, the relevant quantity by the corresponding quantity from an annual cycle of the perturbed (2 × CO_2) integration. Each term in Eqs. (5.7) and (5.8) is then obtained by subtracting the standard values from the corresponding perturbed values. Tables 3 and 4 present the values of the various terms in Eqs. (5.4), (5.7) and (5.8) as computed by this procedure for the GVC and GPC models, respectively. Here, (W m^{-2}) is watts per meter squared. From Eqs. (5.3) and (5.4) we obtain

$$\delta_x\tilde{R} \approx -\delta_T\tilde{R} - \delta_r\tilde{R} - \delta_A\tilde{R} - \delta_c\tilde{R}. \quad (5.9)$$

For the convenience of the present analysis, one can define the feedback parameters λ_T, λ_r, λ_A and λ_c as follows:

$$-\delta_T\tilde{R} = -\left(\sum_i \frac{\partial\tilde{R}}{\partial T_i}\frac{dT_i}{d\tilde{T}_N}\right)\delta\tilde{T}_N \equiv \lambda_T\delta\tilde{T}_N \quad (5.10)$$

TABLE 3. $\delta_v Y$ from the GVC model. Units are W m^{-2}.

	v					
Y	T	r	A	C	X	Σ
$\tilde{S}$	—	1.15	2.20	1.00	0.15	4.50
$-\tilde{F}$	−12.57	5.45	—	0.50	2.07	−4.55
$\tilde{R}$	−12.57	6.60	2.20	1.50	2.22	−0.05

TABLE 4. $\delta_v Y$ from the GPC model. Units are W m^{-2}.

	v					
Y	T	r	A	C	X	Σ
$\tilde{S}$	—	0.77	1.89	—	0.14	2.80
$-\tilde{F}$	−8.36	3.33	—	—	2.08	2.95
$\tilde{R}$	−8.36	4.10	1.89	—	2.22	−0.15

$$-\delta_r\tilde{R} = -\left(\sum_i \frac{\partial\tilde{R}}{\partial r_i}\frac{dr_i}{d\tilde{T}_N}\right)\delta\tilde{T}_N \equiv \lambda_r\delta\tilde{T}_N \quad (5.11)$$

$$-\delta_A\tilde{R} = -\left(\frac{\partial\tilde{R}}{\partial A}\frac{dA}{d\tilde{T}_N}\right)\delta\tilde{T}_N \equiv \lambda_A\delta\tilde{T}_N \quad (5.12)$$

$$-\delta_c\tilde{R} = -\left(\sum_i \frac{\partial\tilde{R}}{\partial C_i}\frac{dC_i}{d\tilde{T}_N}\right)\delta\tilde{T}_N \equiv \lambda_c\delta\tilde{T}_N, \quad (5.13)$$

where i ranges from 1 at the highest to $i = N$ at the lowest of the model atmosphere, and $\tilde{T}_N$ denotes the global mean surface air temperature (i.e., the global mean temperature at the lowest finite difference level located about 70 m above the ground). Here, λ_T, λ_r, λ_A and λ_c are the parameters of temperature-, water vapor-, albedo- and cloud-feedbacks, respectively.

The temperature feedback parameter λ_T may be subdivided into the mean temperature feedback parameter λ_0 and the lapse rate feedback parameter λ_{LR} as follows:

$$\lambda_T \equiv \lambda_0 + \lambda_{LR} \quad (5.14)$$

where

$$\lambda_0 \equiv \frac{d}{d\tilde{T}_N}\epsilon\sigma\tilde{T}_N^4 = 4\epsilon\sigma\tilde{T}_N^3, \quad (5.15)$$

and ϵ is the effective emissivity of the earth–atmosphere system for the upward flux of terrestrial radiation ($\tilde{F} \equiv \epsilon\sigma T_N^4$). From Eq. (5.14), the lapse rate feedback parameter λ_{LR} may be computed as a residual.

Using relationships (5.10), (5.11), (5.12), (5.13) and (5.14), the expression (5.9) becomes

$$\delta_x\tilde{R} = \lambda\delta\tilde{T}_N \quad (5.16)$$

where

$$\lambda \approx \lambda_0 + \lambda_{LR} + \lambda_r + \lambda_A + \lambda_c. \quad (5.17)$$

The Eqs. (5.16) and (5.17) are analogous to the formulation of the feedback effect in the zero dimensional model of Dickinson (1981). As this equation implies, the larger the feedback parameter λ, the smaller is the response of the global mean surface air temperature $\delta\tilde{T}_N$ to the CO_2 radiative forcing $\delta_x\tilde{R}$.

The formulation of the feedback analysis described above differs substantially from that used by Hansen et al. (1984). For example, they used a global mean, one-dimensional model of radiative convective equilibrium to determine the feedback parameters of their three-dimensional model. Although the radiation al-

TABLE 5. Feedback parameters of the GVC and GPC models. Units are in W m^{-2} °C^{-1}.

	λ_0	λ_{LR}	λ_r	λ_A	λ_c	λ	δT_N	$\lambda\delta T_N$	$\delta_x R$
GVC	3.37	−0.23	−1.65	−0.55	−0.37	0.57	4.0	2.28	2.22
GPC	3.37	−0.76	−1.28	−0.59	0	0.74	3.2	2.37	2.22

gorithm used in the one-dimensional model is compatible with that used in their three-dimensional model, the sensitivities of the two models could be significantly different from each other. In particular, it is difficult to determine the global mean cloudiness which has the same radiative effect as the cloudiness in a three-dimensional model. Therefore, it was decided to use the formulation described above rather than their approach.

One should also note that the present analysis uses the fluxes at the top of the model atmosphere rather than those at the tropopause which are commonly used by other studies. This is why $\delta_x F$ in Tables 3 and 4 turned out to be approximately 2 W m^{-2} and is much smaller than 4 W m^{-2} obtained by other studies (for example, see Ramanathan et al. 1979; Hansen et al. 1981; Schlesinger 1986). Since the height of the tropopause is often ill-defined in high latitudes and varies between the standard and high CO_2-experiments, it was decided to choose the top of the model atmosphere as a reference level in the present study.

b. *Feedback parameters*

Table 5 contains the values of the feedback parameters (i.e., λ_0, λ_{LR}, λ_r, λ_A, λ_c) which are computed from Tables 3 and 4. In addition, the values of $\lambda\delta T_N$ and $\delta_x R$ are added to the table to evaluate the approximate expression (5.17).

According to this table, the value of the feedback parameter λ of the GVC-model is significantly smaller than that of the GPC-model, underscoring the difference in sensitivity between the two models. In both models, λ_A is negative. This indicates the positive feedback effect of snow and sea ice. Since the values of λ_A are similar in these models, the albedo feedback process does not account for the difference in λ between the two models.

This table also indicates that λ_c is negative in the GVC-model implying that the cloud-induced change of radiative fluxes at the top of the model atmosphere is a positive feedback process. Obviously, λ_c is zero in the GPC-model without the cloud feedback process. The magnitude of the difference in λ_c between the two models is more than that of the difference in λ mentioned above.

The lapse-rate feedback parameter λ_{LR} is negative in both models because of the reversal of the sign of the CO_2-induced temperature change between the troposphere and the stratosphere of the models. Here λ_{LR} of the GVC model is −0.23 W m^{-2} °C^{-1} and is significantly different from the λ_{LR} of the GPC model, which is −0.76 W m^{-2} °C^{-1}. The CO_2-induced change of cloud cover results in the change in the radiative heating (or cooling) and stabilizes the model troposphere thereby increasing the feedback parameter ($\lambda_T + \lambda_r$). To demonstrate this process, the influence of the CO_2-induced change of cloud cover upon the radiative heating (or cooling) in the GVC atmosphere is determined. This was done by computing the rate of radiative temperature change in the model atmosphere for the two time series of daily cloudiness obtained from the ($2 \times CO_2$) and ($1 \times CO_2$) integrations of the GVC model. All other relevant fields required for the computation of the radiative transfer processes are obtained from the $1 \times CO_2$ integration of the GVC model. The difference between the two rates thus computed is averaged both zonally and annually and shown in Fig. 12. In this figure, one can identify the thick layer of positive change around the tropopause of middle and low latitudes where the radiative cooling is reduced significantly due to the CO_2-induced increase of cloud amount. However, the influence of the CO_2-induced change of cloudiness upon the radiative temperature change is small in the rest of the troposphere with the exception of the surface layer where it has a positive value of significant magnitude. It is expected that these radiative changes increase the static stability of the GVC troposphere.

In order to compare the change in static stability between the two models, the following quantity is computed for both the GVC and GPC atmospheres.

$$\delta\tilde{T}(\theta, p)/\delta\tilde{T}_N \tag{5.18}$$

where

$$\delta = (\ )_{2x} - (\ )_{1x} \tag{5.19}$$

and θ and p are latitude and pressure respectively, and $\tilde{T}_N$ denotes the global mean surface air temperature obtained from each model. This quantity denotes the change in zonal mean temperature of the model atmosphere which accompanies a unit increase of the global mean surface temperature. Figure 13 illustrates the latitude–height distribution of the zonal mean difference of these ratios between the two models (i.e., GVC − GPC models). It is indicated that the increase of the static stability of the troposphere accompanying a unit increase of global mean surface air temperature is larger in the GVC than the GPC model. Such a stabilization increases the upward flux of terrestrial ra-

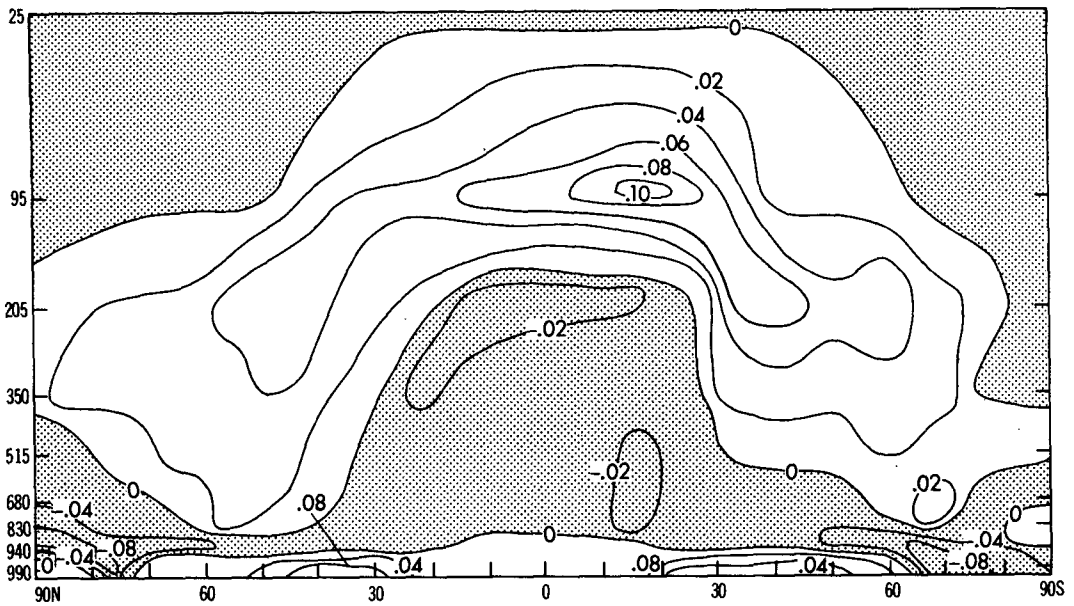

FIG. 12. Latitude-height distribution of the zonal mean value of δ_c (rate of radiation temperature change) in the GVC atmosphere. Units are in °C day^{-1}. Here, δ_c( ) denotes the influence of the CO_2 induced change of cloud cover upon the rate of radiative temperature change.

diation at the top of a model atmosphere making λ_{LR} less negative. Thus, the parameter of the temperature feedback $\lambda_T = \lambda_0 + \lambda_{LR}$ is 3.14 W m^{-2} °C^{-1} for the GVC model and is larger than the value of 2.61 W m^{-2} °C^{-1} obtained from the GPC model.

The change of static stability of the GVC model described above also induces a change in the vertical distribution of water vapor. Accordingly, the value of λ_r is -1.65 W m^{-2} °C^{-1} in the GVC model and is significantly different from -1.28 W m^{-2} °C^{-1} of the GPC model. Although the difference in λ_r between the two models partially offsets the difference in λ_{LR}, the ($\lambda_0 + \lambda_{LR} + \lambda_r$)-value of the GVC model is still larger than that of the GPC model. Summing up all contributions

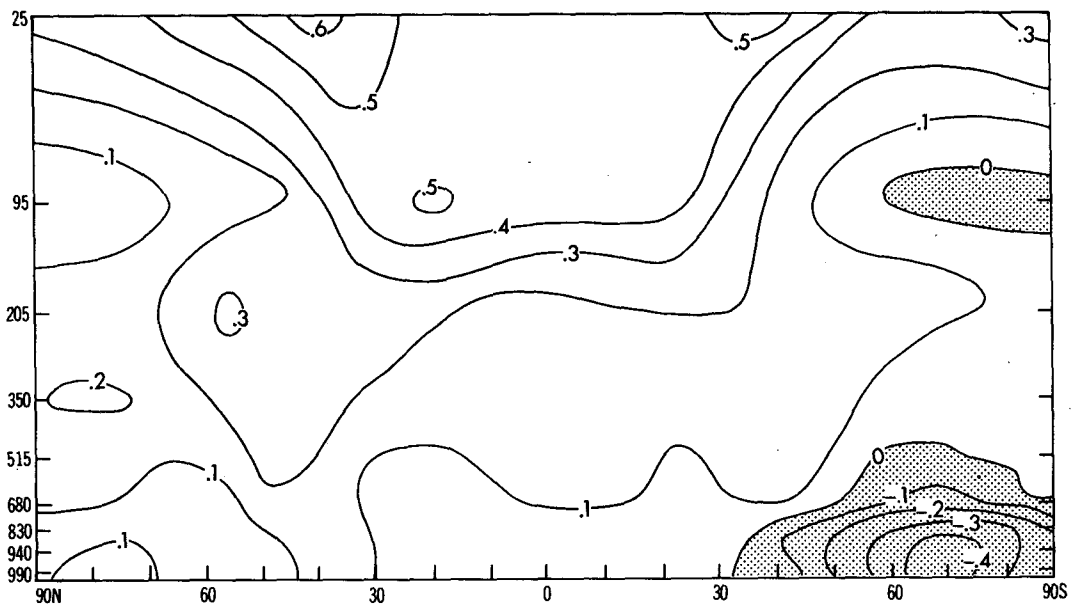

FIG. 13. Latitude-height distribution of the difference of the ratio defined by Eq. (5.18) between the GVC and GPC models.

listed in the right hand side of the Eq. (5.17), the λ-value of the GVC model is smaller than that of the GPC model indicating that the net effect of the CO_2-induced change of cloudiness is the enhancement of the sensitivity of a model climate.

In summary, the CO_2-induced change of cloud cover alters the radiative flux at the top of the atmosphere of the GVC model enhancing its sensitivity. However, the change of cloud cover also modifies the distribution of radiative heating (or cooling) in the GVC atmosphere, thereby increasing the static stability and inducing the change of the vertical water vapor distribution in the model troposphere. These tropospheric changes partially offset the positive feedback effect of the radiative flux change at the top of the model atmosphere mentioned above. The net effect of the CO_2-induced change of cloudiness is to enhance the sensitivity of the model climate. Thus the increase of the global mean surface air temperature of the GVC model in response to the CO_2-doubling is 4.0°C which is substantially larger than the warming of 3.2°C of the GPC model.

c. *Cloud-induced changes in radiative fluxes*

It has been shown that the change in the atmospheric transfer of radiation resulting from the change of the cloud distribution enhances the sensitivity of climate of the GVC model. To determine the mechanism involved in this positive feedback process the cloud-induced changes of radiative flux at the top of the model atmosphere are subdivided into two parts as

$$\delta_c\bar{S} = \delta_{cA}\bar{S} + \delta_{cH}\bar{S} \tag{5.20}$$

$$\delta_c\bar{F} = \delta_{cA}\bar{F} + \delta_{cH}\bar{F} \tag{5.21}$$

where S and F are net downward flux of solar radiation and upward flux of terrestrial radiation at the top of the atmosphere, respectively. The $\delta_{cA}\bar{Y}$ and $\delta_{cH}\bar{Y}$ denote zonal mean change of flux Y due to changes in the amount and height of cloud cover, respectively. Here, $\delta_{cA}\bar{Y}$ is defined by the following equation.

$$\delta_{cA}\bar{Y} \equiv \Delta_c\bar{Y}\frac{\delta\bar{C}_T}{\bar{C}_T} \tag{5.22}$$

where $\Delta_c Y$ is the influence of cloud cover upon a radiative flux at the top of the atmosphere (Y), i.e.,

$$\Delta_c Y = Y(x, T_i, r_i, A, c_i) - Y(x, T_i, r_i, A, 0), \tag{5.23}$$

and C_T and δC_T are total cloudiness (i.e., the fraction of cloud coverage as seen from the top of the atmosphere) and its change caused by the doubling of atmospheric carbon dioxide. $\Delta_c Y$ is called "cloud forcing" by Ramanathan (1987) and represents the difference in Y between a cloudy and a hypothetically clear atmosphere. Given $\delta_{cA}Y$, $\delta_{cH}Y$ may be computed from the following equation

$$\delta_{cH}\bar{Y} = \delta_c\bar{Y} - \delta_{cA}\bar{Y}. \tag{5.24}$$

Figures 14a and 14b illustrate the latitudinal distributions of the changes of the radiative flux which are attributable to the CO_2-induced changes in the amount and height of cloud. The changes of solar fluxes $\delta_c\bar{S}$, $\delta_{cA}\bar{S}$ and $\delta_{cH}\bar{S}$ are shown in Fig. 14a and those of terrestrial fluxes $\delta_c\bar{F}$, $\delta_{cA}\bar{F}$ and $\delta_{cH}\bar{F}$ are contained in Fig. 14b.

As described earlier, cloudiness is reduced in the thick layer of the upper troposphere and increases around the tropopause of the model in low latitudes. The reduction of planetary albedo due to the upper tropospheric decrease of cloudiness substantially exceeds the contribution from the increased cloudiness around the tropopause, thereby increasing the net incoming solar radiation. This explains why $\delta_{cA}S$ is positive in low latitudes (30°S ~ 40°N). In middle to high latitudes, the increase of cloud amount in the surface layer and around the tropopause increases the planetary albedo and makes $\delta_{cA}\bar{S}$ negative in these regions of both hemispheres. When $\delta_{cA}\bar{S}$ is averaged over the entire global domain, the contribution from the positive values in the low latitudes substantially exceeds that from the negative values of high latitudes. Thus, the global mean value of $\delta_{cA}\bar{S}$ is 0.64 W m^{-2} as indicated in Table 6.

According to Fig. 14a, $\delta_{cH}\bar{S}$ has a small positive value at most latitudes. When $\delta_{cH}\bar{S}$ is averaged over the global domain, $\delta_{cH}S$ is 0.34 W m^{-2} and is substantially smaller than $\delta_{cA}\bar{S}$ as discussed in the preceding paragraph. Adding $\delta_{cA}\bar{S}$ and $\delta_{cH}\bar{S}$ one obtains a $\delta_c\bar{S}$-value of 1.00 W m^{-2} as indicated by Table 6.

The latitudinal profiles of the cloud induced changes of the upward flux of terrestrial radiation at the top of the model atmosphere (i.e., $\delta_c\bar{F}$, $\delta_{cA}\bar{F}$ and $\delta_{cH}\bar{F}$) are shown in Fig. 14b. Note here that positive ($\bar{F}$) is taken as upward flux so that positive ($-\delta_v\bar{F}$) represents a heat gain for the atmospheric surface system.

It is of interest that $-\delta_{cH}\bar{F}$ is positive at most latitudes. In response to the doubling of the atmospheric concentration of carbon dioxide, cloudiness increases around the tropopause and is reduced in the upper troposphere of the model. Thus, the upper tropospheric layer of relatively large cloudiness shifts upward as discussed in section 4. The rise of high cloud contributes to the reduction of the upward terrestrial radiation at the top of the model atmosphere at most latitudes. Thus, $-\delta_{cH}\bar{F}$, (i.e., the global mean value of $\delta_{cH}\bar{F}$) has a positive value of 0.66 W m^{-2} which enhances the CO_2-induced warming of the combined atmosphere–earth surface system.

Figure 14b also indicates that $-\delta_{cA}\bar{F}$ is negative in low latitudes and is positive in high latitudes. Because of the reduction of cloud amount (Fig. 7) the effective emission temperature of the outgoing radiation increases resulting in the negative $-\delta_{cA}\bar{F}$ in low latitudes. On the other hand, the increase of cloud amount lowers

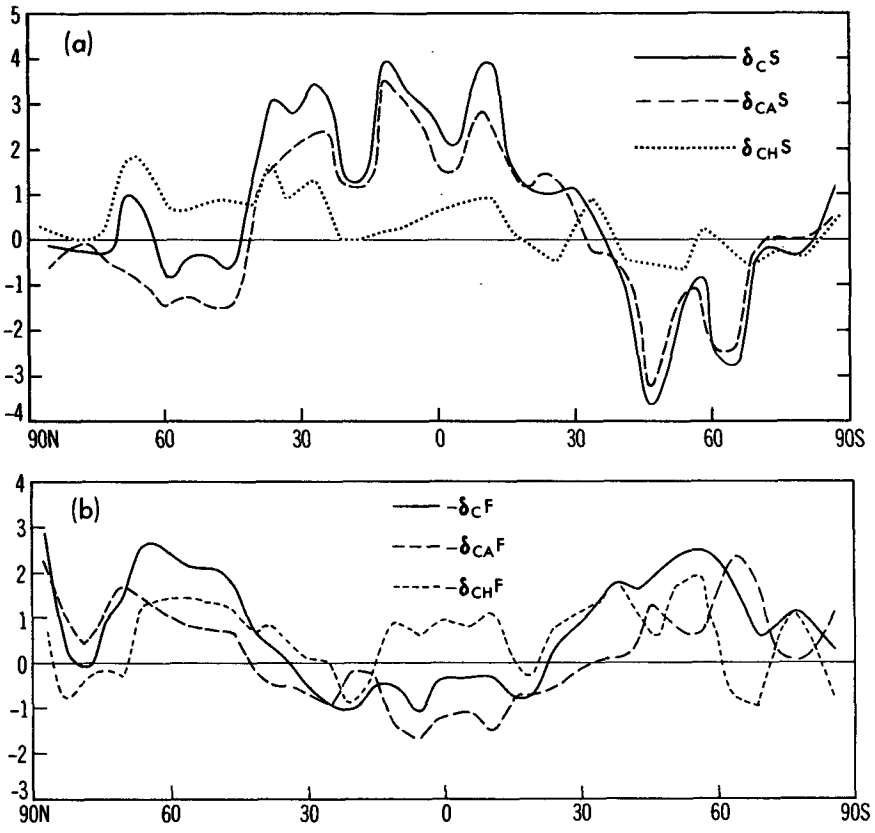

FIG. 14. Latitudinal distributions of (a) $\delta_c S$, $\delta_{cA} S$ and $\delta_{cH} S$, (b) $-\delta_c F$, $-\delta_{cA} F$ and $-\delta_{cH} F$ for the GVC model. Units are W m^{-2}.

the effective emission temperature for the outgoing radiation accounting for the positive $-\delta_{cA}\bar{F}$ in high latitudes. Since the negative contribution from the low latitudes slightly exceeds the positive contribution from the high latitudes, $-\delta_{cA}\tilde{F}$ (i.e., the global mean value of $\delta_{cA}\bar{F}$) has a small negative value of -0.16 W m^{-2} as indicated by Table 4.

In summary, the increase of the net incoming solar radiation and the reduction of the outgoing terrestrial radiation at the top of the model atmosphere, which result from the change in cloud cover, enhance the CO_2-induced warming of the coupled troposphere–mixed-layer ocean system of the model.

TABLE 6. Cloud-induced changes in global mean radiative fluxes ($\delta_v Y$). Units are in W m^{-2}.

	v		
Y	cA	cH	c
$\tilde{S}$	0.64	0.34	1.00
$-\tilde{F}$	−0.16	0.66	0.50
$\tilde{R}$	0.48	1.02	1.50

6. Comparison with previous results

The results presented in the preceding section suggest that the interaction between cloud cover and radiation enhances the CO_2-induced warming of climate and is a positive feedback process. This suggestion is different from that obtained from the earlier studies by the present authors (Wetherald and Manabe 1980; Manabe and Wetherald 1980) which suggested that the cloud feedback process has very little influence upon the sensitivity of climate. In both present and earlier studies, cloud amount increases around the tropopause and is reduced in the upper troposphere at most latitudes in response to an increase of atmospheric carbon dioxide (or solar constant). Another common feature of the CO_2-induced change of cloud cover is the increase of cloud amount in the surface layer of high latitudes. The magnitudes of these changes, however, are significantly different between the present and earlier studies. For example, the increase of cloud amount around the tropopause in low latitudes was very small in the earlier studies, whereas it has a significant magnitude in the present study. Also, the increase of cloud amount in the surface layer of high latitudes in the earlier studies is larger than the increase in the present study. These

quantitative differences in the CO_2-induced change of cloud cover are partly responsible for the difference in climate sensitivity between the earlier and the present results as described below.

In both earlier and present studies, cloud cover increased around the tropopause and in the surface layer at high latitudes. However, this increase of cloudiness in high latitudes is considerably greater in the earlier study than in the present one. One should also note that, in the present study, the low cloudiness is actually reduced in summer when the insolation is at a maximum as described in section 4b. Thus, the negative feedback process involving solar radiation and cloud cover in high latitudes is smaller in the present study.

One of the other relevant factors is the above mentioned difference in the CO_2-induced change of cloud amount around the tropopause in low latitudes. This difference accounts for the fact that, because of the CO_2-induced change of the cloud distribution, the effective source temperature of the upward terrestrial radiation increases in the earlier study whereas it is significantly reduced in the present study enhancing the positive feedback effect of cloud cover.

It is not entirely clear why the CO_2-induced change of cloud cover is different between the present and earlier studies. One should note, however, that many simplifications were made in the construction of the model used in the earlier studies because of the limitation of computer capability. For example, the model had an idealized sector geography and an annually averaged insolation which does not change with season. It applies an energy-conserving finite difference method to the regular grid system with the grid size of approximately 500 km. The model incorporates nonlinear subgrid-scale mixing of momentum, heat and moisture. It has been recognized that the subgrid-scale viscosity of this model is substantially larger than that of the present model which employs a semispectral technique and biharmonic subgrid-scale mixing. To identify the factors responsible for the differences in behavior between the earlier and present models, a series of sensitivity studies has been conducted after modifying the present model in various ways. For example, both GVC and GPC models are modified such that they have an annually averaged rather than seasonally varying insolation. By comparing the sensitivities of the modified models with those of the original models, it was found that the positive feedback effect of cloud cover in the modified annual model is half as large as that in the original GVC model. In this modified model, the change of cloud amount around the tropopause in low latitudes remains significant despite the removal of the seasonal variation of insolation. However, the CO_2-induced increase of near-surface cloud is larger than the corresponding increase in the original seasonal model, thereby weakening the overall positive feedback process of cloud cover. This explains approximately half of the difference in the magnitude of the cloud feedback effect between the present and the earlier models.

In the next set of experiments, the GVC and GPC models are modified such that they have not only annually averaged insolation but also the idealized sector-geography of the earlier model. According to the results from these modified models, the influence of the cloud feedback process upon the sensitivity of the model climate is similar to the global model with annual mean insolation, but is, again, half as large as the original global GVC model with seasonally varying insolation. This result suggests that the idealization of geography is not responsible for the small cloud feedback effect of the earlier model.

In order to explain satisfactorily the difference in sensitivity between the present GVC model and the earlier model, it is necessary to explain why the CO_2-induced change of cloud cover around the tropical tropopause is different between the two models. It is possible that the cloud change may depend critically upon the choice of finite difference levels particularly around the tropopause where the water vapor content and static stability vary sharply with increasing altitude. The second finite difference level is located around 95 mb in the present GVC model whereas it is located around 70 mb in the earlier model. Further numerical experiments are required to confirm this speculation.

Recently, Wetherald and Manabe (1986) compared the CO_2-induced changes of cloud cover obtained from several models constructed by different groups: (Hansen et al. 1984; Washington and Meehl 1984). According to this comparison, there is a tendency for cloud amount to increase around the tropopause poleward of tropical latitudes in both of these models in agreement with the present results. However, neither model indicates a positive cloud change around the tropical tropopause. This is due to the fact that no clouds are allowed to form at the top two finite difference levels in either the Hansen et al. model (Hansen et al. 1983) or the Washington and Meehl model (Ramanathan et al. 1983). This assumption precludes the potential increase of cloudiness around the tropical tropopause in these two models. Therefore those authors' results in this region appear to differ from the present result. It is difficult to assess the impact of this assumption upon the cloud change in the experiment of Washington and Meehl because the information on the change of relative humidity is not available. In the experiment of Hansen et al. an increase of relative humidity is indicated around the tropical tropopause (Rind, personal communication). Therefore, it is probable that, in qualitative agreement with the present result, a corresponding increase of cloud amount would have occurred if this assumption had not been adopted. Furthermore, the latest experiments conducted by Wilson et al. (1986) also indicate an increase of cloud

amount around the tropical tropopause. In fact, the general pattern of cloud change obtained from their model is in reasonable agreement with that from the present study. This result, together with the cloud changes from the other more recent cloud prediction experiments conducted at GFDL, imply that the pattern of cloud change obtained from the present study is probably more reliable than those from our earlier investigations with idealized geography.

7. Summary and conclusions

The CO_2-induced changes of cloud cover obtained from the present experiment are qualitatively (but not quantitatively) similar to the changes from other models developed at GFDL and other institutions (Wetherald and Manabe 1980; Hansen et al. 1984; Washington and Meehl 1984). This was noted in a review paper by Wetherald and Manabe (1986). Some of these changes are 1) the reduction of cloud amount in the upper troposphere, 2) an increase of cloud amount around the tropopause and 3) an increase of cloud amount near the earth's surface in high latitudes. Both the increase of cloud amount around the tropopause and its reduction in the upper troposphere are the manifestation of the upward shift of the relatively stable layer of large cloudiness where rising, saturated air tends to spread horizontally. Since the heating due to moist convection intensifies in middle and low latitude in response to an increase of atmospheric carbon dioxide, the tropospheric layer of relatively low, moist static stability extends to a higher altitude and causes this upward shift of high cloud.

It is found that the interaction between cloud cover and radiation is a positive feedback process in the present model enhancing the CO_2-induced warming of the model troposphere. The increase of global mean surface air temperature due to the doubling of the atmospheric carbon dioxide is 4.0° and 3.2°C with and without the cloud feedback process. The present result is in qualitative agreement with the result obtained by Hansen et al. (1984). However, the positive feedback effect of cloud cover in the present model appears to be much weaker than that in their model.

In order to elucidate the physical mechanisms involved in this positive feedback process, the results from the present numerical experiment are analyzed in detail. According to this analysis, both solar and terrestrial radiation are affected substantially by the change of cloud cover and enhance the CO_2-induced warming of the model climate. For example, the effective source temperature of the outgoing terrestrial radiation is reduced due to the rise of the high cloud layer mentioned above. Thus, the loss of heat due to the outgoing radiation is reduced thereby enhancing the CO_2 warming of the model climate.

The change in the distribution of high cloud not only lowers the heat loss by outgoing terrestrial radiation but also increases the heat gain due to the absorption of solar radiation. In the upper model troposphere, the vertical profile of cloudiness is significantly altered as the layer of high cloud moves upward in response to the doubling of the atmospheric carbon dioxide. For example, the magnitude of the upper tropospheric reduction of cloudiness is significantly larger than the corresponding increase of cloud amount around the tropopause in low latitudes. Thus, the reduction of planetary albedo due to the former change of cloud overshadows the albedo increase due to the latter change. The increase of solar absorption resulting from the net reduction of planetary albedo enhances the CO_2-induced warming of the model climate.

The upward shift of high cloud described above has another implication. By altering the vertical distribution of radiative temperature change, such a shift increases the static stability of the model atmosphere. As discussed by Held (1978), a stabilization of the atmosphere reduces the sensitivity of surface air temperature by reducing the change of outgoing terrestrial radiation accompanying a given change of surface air temperature. However, this effect is smaller than the direct positive feedback effect of cloud cover described in the preceding paragraphs. Thus, the net contribution from the upward shift of high cloud is an enhancement of CO_2-induced warming.

Another feature of the CO_2-induced change of cloud cover identified earlier is the increase of low cloudiness in high latitudes. This raises the planetary albedo without significantly affecting the outgoing terrestrial radiation at the top of the model atmosphere. Thus, the CO_2-induced warming of climate is reduced. The contribution from this low cloud change is much smaller than the contribution from the upward shift of high cloud described earlier. This is partly because the low cloud change is large in high latitudes only during winter when the insolation is small.

In summary, the positive feedback effect of high cloud overshadows the smaller negative feedback effect of low cloud in high latitudes. Thus, the cloud process in the present model is positive as stated earlier.

The present study differs from the earlier study by the same authors (Wetherald and Manabe 1980) which suggested that the cloud feedback process does not affect significantly the sensitivity of climate. This is partly because the negative feedback effect involving the stratus cloud in the present seasonal model is significantly smaller than that of the earlier model with the annually averaged insolation. The difference is also attributable to the larger CO_2-induced increase of cloudiness around the tropical tropopause in the present model as compared with the results from the earlier study. Unfortunately, the numerical computation of vertical moisture transport in both studies suffers from large truncation errors in the upper model troposphere where the moisture content of air decreases rapidly with in-

creasing altitude. Furthermore, the vertical distribution of low cloudiness is poorly resolved in these models. Therefore, it is highly desirable to repeat the present study with a model which has greater vertical resolution for the finite difference computation than the present one.

There are indications that the change of cloud cover obtained from a sensitivity study may significantly depend upon the method chosen for the parameterization of moist convection. For example, the Washington and Meehl (1984) and the present models employ the moist convective adjustment scheme proposed by Manabe et al. (1965), whereas the models of Hansen et al. (1984) and Wilson et al. (1986) utilize a deep penetrative convection scheme. The latter two studies yield reductions of upper tropospheric cloud cover in the tropical regions that are considerably greater than those given by the first two studies. A comparison of the models reviewed by Schlesinger and Mitchell (1987) and the model developed by Wilson et al. (1986) reveals that the two studies with penetrative convection parameterizations yield greater cloud reductions accompanied by larger temperature increases in the upper model troposphere. Therefore, it is probable that the specific details of the parameterization of moist convection processes can greatly affect the changes of temperature and cloud amount in the upper model troposphere which, in turn, can have a significant effect upon the sensitivity of a model climate.

Before concluding this paper, it is important to note the recent study of Somerville and Remer (1984). They suggested that accompanying the CO_2-induced warming of the atmosphere, the liquid water content of cloud may increase, thereby increasing the planetary albedo. Such a negative feedback process can oppose the positive feedback effect described in this study.

In view of the extreme idealizations made in the parameterization of the cloud-radiation interaction, the present study should be regarded as a qualitative study of the cloud feedback process rather than a quantitative assessment of the influence of this process upon the sensitivity of climate. To reduce the large uncertainty in the current estimate of climate sensitivity, a major effort should be devoted to improve the treatment of the cloud feedback process in climate models. In particular, a model should reproduce with sufficient fidelity the horizontal distributions of cloud amount and radiative fluxes as determined by satellite observations. Other research topics, which require immediate attention, include the dependence of liquid water content in cloud upon temperature and other relevant variables.

Acknowledgments. The authors would like to thank V. Ramaswamy, S. Fels and J. Mahlman for their constructive remarks on a preliminary version of the manuscript. They also wish to express an appreciation to M. Schlesinger for his in-depth and thorough review of our study. Finally, they thank J. Kennedy and P. Tunison and his staff for preparing the final version of the manuscript and illustrations.

REFERENCES

Berlyand, T. G., L. A. Strokina and L. E. Greshnikova, 1980: Zonal cloud distribution on the earth. *Meteor. Gidrol.*, **3**, 15–23.

Bryan, K., 1969: Climate and ocean circulation. II. The ocean model. *Mon. Wea. Rev.*, **97**, 828–829.

Cess, R. D., 1976: Climate change: An appraisal of atmospheric feedback mechanisms employing zonal climatology. *J. Atmos. Sci.*, **33**, 1831–1843.

Crutcher, H. L., and J. M. Meserve, 1970: Selected level heights, temperatures, and dew points for the Northern Hemisphere. Rep. NAVAIR 50-IC-52, U.S. Naval Weather Service, Washington, DC.

Dickinson, R. E., 1981: Convergence rate and stability of ocean-atmosphere coupling schemes with a zero-dimensional climate model. *J. Atmos. Sci.*, **38**, 2112–2120.

Ellis, J. S., and T. H. Vonder Haar, 1976: Zonal average earth radiation budget measurements from satellites for climate studies. Atmos. Sci. Paper No. 240, Colorado State University.

Gordon, C. T., and W. F. Stern, 1982: A description of the GFDL global spectral model. *Mon. Wea. Rev.*, **110**, 625–644.

Hansen, J., D. Johnson, A. Lacis, S. Lebedeff, P. Lee, D. Rind and G. Russell, 1981: Climate impact of increasing atmospheric carbon dioxide. *Science*, **213**, 957–966.

——, A. Lacis, D. Rind, G. Russel, P. Stone, I. Fung, R. Ruedy and J. Lerner, 1984: Climate sensitivity: Analysis of feedback mechanisms. *Climate Process and Climate Sensitivity*, Maurice Ewing Series (5), J. E. Hansen, and T. Takahashi Eds., Amer. Geophys. Union, 130–163.

——, G. Russell, D. Rind, P. Stone, A. Lacis, S. Lebedeff, R. Ruedy and L. Travis, 1983: Efficient three-dimensional global models for climate studies: Models I and II. *Mon. Wea. Rev.*, **111**, 609–662.

Hartmann, D. L., and D. A. Short, 1980: On the use of earth radiation budget statistics for studies of clouds and climate. *J. Atmos. Sci.*, **37**, 1233–1250.

Held, I. M., 1978: The tropospheric lapse rate and climate sensitivity: Experiments with a two-level atmospheric model. *J. Atmos. Sci.*, **35**, 2083–2098.

Holton, J. R., 1979: *An Introduction to Dynamic Meteorology*, second ed. Academic Press, 391 pp.

Kondratiev, K. Ya., 1972: Radiation processes in the atmosphere. WMO-No. 309. 214 p. World Meteorological Organization, Geneva.

Lacis, A. A., and J. E. Hansen, 1974: A parameterization for the absorption of solar radiation in the earth's atmosphere. *J. Atmos. Sci.*, **31**, 118–133.

Manabe, S., 1969: Climate and ocean circulation. I. The atmospheric circulation and the hydrology of the earth's surface. *Mon. Wea. Rev.*; **97**, 739–774.

——, and R. T. Wetherald, 1967: Thermal equilibrium of the atmosphere with a given distribution of relative humidity. *J. Atmos. Sci.*, **24**, 241–259.

——, and ——, 1975: The effects of doubling of the CO_2 concentration on the climate of a general circulation model. *J. Atmos. Sci.*, **37**, 99–118.

——, and ——, 1980: Sensitivity of a global climate model to an increase of CO_2 concentration in the atmosphere. *J. Geophys. Res.*, **85**, 5529–5554.

——, and R. T. Wetherald, 1980: On the distribution of climate change resulting from an increase in CO_2 content of the atmosphere. *J. Atmos. Sci.*, **37**, 99–118.

——, and ——, 1982: Simulation of global cloud cover. World Climate Program Rep. No. 34. WMO, Geneva. 241–259.

——, and A. J. Broccoli, 1985: A comparison of climate model sensitivity with data from the last glacial maximum. *J. Atmos. Sci.*, **42**, 2643–2651.

——, and R. T. Wetherald, 1987: Large scale changes of soil wetness induced by an increase in atmospheric carbon dioxide. *J. Atmos. Sci.*, **44**, 1211–1235.

——, J. Smagorinsky and R. F. Strickler, 1965: Simulated climatology of a general circulation model with a hydrologic cycle. *Mon. Wea. Rev.*, **93**, 769–798.

Ohring, G., and P. F. Clapp, 1980: The effect of change in cloud amount on the net radiation at the top of the atmosphere. *J. Atmos. Sci.*, **37**, 447–454.

Orsag, S. A., 1970: Transform method for calculation of vector-coupled sums: Application to the spectral form of the vorticity equation. *J. Atmos. Sci.*, **27**, 890–895.

Ramanathan, V., 1987: The role of earth radiation budget studies in climate and general circulation research. *J. Geophys. Res.*, **92**, 4075–4095.

——, M. S. Lian, and R. D. Cess, 1979: Increased atmospheric CO_2: Zonal and seasonal estimates of the effects on the radiation energy balance and surface temperature. *J. Geophys., Res.*, **84**, 4949–4958.

——, E. J. Pitcher, R. C. Malone and M. L. Blackmon, 1983: The response of a spectral general circulation model to refinements in radiative processes. *J. Atmos. Sci.*, **40**, 605–630.

Rodgers, C. D., 1967: The radiative heat budget of the troposphere and lower stratosphere. Planetary Circulation Project, Rep. No. A2, Massachusetts Institute of Technology, Cambridge, Ma. 104 pp. NTIS PB-176 527.

——, and C. D. Walshaw, 1966: The computation of infrared cooling rate in planetary atmospheres. *Quart. J. Roy. Meteor. Soc.*, **92**, 67–92.

Schlesinger, M. E., 1986: Equilibrium and transient climatic warming induced by increased atmospheric CO_2. *Climate Dyn.*, **1**, 35–51.

——, and J. F. B. Mitchell, 1987: Model projections of the equilibrium climatic response to increased CO_2. *Rev. Geophys.*, **25**, 760–798.

Schneider, S. H., 1972: Cloudiness as a global climate feedback mechanism: The effects on the radiation balance and surface temperature of variations in cloudiness. *J. Atmos. Sci.*, **29**, 1413–1422.

Somerville, R. C., and L. A. Remer, 1984: Cloud optical thickness feedbacks in the CO_2 climate problem. *J. Geophys. Res.*, **89**(D6), 9668–9672.

Taljaard, J. J., H. van Loon, H. L. Crutcher and R. L. Jenne, 1969: Climate of the upper air, 1, Southern Hemisphere. Rep. NAVAIR 50-IC-55, U.S. Naval Weather Service, Washington, DC.

Washington, W. M., and G. A. Meehl, 1984: Seasonal cycle experiments on the climate sensitivity due to a doubling of CO_2 with an atmospheric general circulation model coupled to a simple mixed layer ocean model. *J. Geophys. Res.*, **89**(D6), 9475–9503.

Wetherald, R. T., and S. Manabe, 1980: Cloud cover and climate sensitivity. *J. Atmos. Sci.*, **37**, 1485–1510.

——, and ——, 1986: An investigation of cloud cover change in response to thermal forcing. *Clim. Change*, **8**, 5–23.

Wilson, C. A., J. F. B. Mitchell and W. M. Cunnington, 1986: 2 $\times CO_2$ climate sensitivity experiment with a global climate model including a simple ocean. EEC Contract Rep., CL-1141-UK(H).